Investigation of Phase Formation and Electrical Properties of Fe-Doped PZT Ceramics

Alina Iulia DUMITRU
National Institute for Research & Development in Electrical Engineering ICPE-CAaNational Institute for Research & Development in Electrical Engineering ICPE-CA

Georgeta VELCIU
National Institute for Research & Development in Electrical Engineering ICPE-CAaNational Institute for Research & Development in Electrical Engineering ICPE-CA

Delia PATROI
National Institute for Research & Development in Electrical Engineering ICPE-CAaNational Institute for Research & Development in Electrical Engineering ICPE-CA

Jana PINTEA
National Institute for Research & Development in Electrical Engineering ICPE-CAaNational Institute for Research & Development in Electrical Engineering ICPE-CA

Virgil MARINESCU
National Institute for Research & Development in Electrical Engineering ICPE-CAaNational Institute for Research & Development in Electrical Engineering ICPE-CA

Tudor-Gabriel DUMITRU
University of Bucharest, Faculty of Physics

Ildiko Peter (ildiko.peter@umfst.ro)
University of Medicine https://orcid.org/0000-0003-3484-8475

Research Article

Keywords: doped PZT, dielectric properties, piezoelectric properties, ferroelectric properties

Posted Date: July 15th, 2021

DOI: https://doi.org/10.21203/rs.3.rs-703468/v1

Abstract

In this paper, some compositions described by the general formula $Pb(Zr_xTi_{1-x})_{0.99}Fe_{0.01}O_3$ have been considered and investigated. The compositions considered have been obtained by solid state reaction technique, where x corresponds to 0.42, 0.52 and 0.58. Sintering has been performed for 2 hours at temperatures between 1100^{o}C and 1250^{o}C. The influence of the sintering temperature on the microstructure and on the hysteresis loops of Fe^{3+} doped $Pb(Zr_xTi_{1-x})O_3$ system has been investigated. The crystallographic phase and microstucture of the sintered compositions have been studied in detail using X-ray diffraction analysis (XRD) and Scanning Electron Microscopy (SEM). The experimental results obtained by XRD have revealed that all the sintered samples have a perovskite structure. In order to correlate the behavior of the sintered materials to their microscopic structure, the domain structures have been defined by SEM. The dielectric properties, as relative dielectric permittivity (ε_r) and dielectric loss (tan δ) have been measured. The hysteresis loops at room temperature of all un-poled sintered compositions reveal a similar behaviour with “hard” PZT ceramics. The piezoelectric properties like electromechanical coupling factor (k_p) have been investigated after polarization.

1 Introduction

Lead zirconate titanate (PZT) ceramic is very attractive material for its properties designing. Wide range of electrical/ piezoelectrical/ ferroelectrical properties can be obtained varying the Zr/Ti ratio, particularly in a so-called morphotropic phase boundary (MPB) region.

PZT materials are almost always used with one or more dopants to improve and optimize their basic properties for specific applications [1, 2]. Acceptor dopants, such as Fe^{3+} replacing (Zr^{4+}, Ti^{4+}), are compensated by oxygen vacancies and usually have a limited solubility in the lattice. Domains reorientation are limited and compositions with acceptor dopants are more difficult to pole and usually are characterized by poorly developed hysteresis loops, low dielectric losses, lower dielectric constant, low piezoelectric properties, higher ageing rate. These materials are called “Hard PZT” [1].

Four compositional regions of $PbZr_xTi_{1-x}O_3$ solid solution can be classified accordingly to their properties and applications [3]:

In the first region with $0 < 1-x < 0.1$ the antiferroelectric and rhombic phase exists at the normal conditions. The antiferroelectric to ferroelectric phase transitions induced by external electric field are used in applications. Materials based on these compositions are used for memory shape applications due to relatively high coefficients of electroelasticity. Another interesting application of these materials is fabrication of elements with high electron emission obtained during phase transition ferroelectric – antiferroelectric controlled by mechanical stress and external electric field [4].

In the second region with $0.1 < 1-x < 0.4$ there are two rhombohedral phases. These compositions reveal high pyroelectric properties used in pyroelectric detectors. Another feature of these compositions with

dopants are states of metastable polarization, which is typical for relaxors [5]. These materials are used in electromechanical transducers and surface acoustic wave devices.

The third region with $0.4 < 1\text{-}x < 0.6$ is the region of solid solutions that includes the morphotropic phase boundary (MPB) separating the rhombohedral region by the tetragonal region, where the crystalline structure and properties are very sensitive to the fluctuation of composition. The structural studies of ferroelectric PZT with Zr/Ti = 52/48, have presented a monoclinic phase in the vicinity of the MPB [6, 7]. In this region, most of the properties are very pronounced and reach the maximum values. These values are used in applications of these materials [8, 9].

In the last region with $0.6 < 1\text{-}x < 1.0$ compositions in wide range of the solid solutions with tetragonal crystalline structure present relatively high anisotropy of piezoelectric coefficients d_{33} and d_{31} and corresponding electromechanical coupling factors k_t and k_p [10]. Other features of these compositions are relatively high coercive fields and high spontaneous deformations. Some applications of these materials include filters and frequency stabilizers.

In this study, three compositions with a general formula, $Pb(Zr_xTi_{1-x})_{0.99}Fe_{0.01}O_3$, have been considered and investigated. The compositions have been chosen as follows: one in the tetragonal region corresponding to Zr/Ti = 42/58 (noted PZTF-42), the second one in the MPB region corresponding to Zr/Ti = 52/48 (noted PZTF-52) while the third one in the rhombohedral region corresponding to Zr/Ti = 58/42(noted PZTF-58).

2 Materials And Methods

Polycrystalline samples of a new ferroelectric compositions with a general formula $Pb(Zr_xTi_{1-x})_{0.99}Fe_{0.01}O_3$ with x having the values 0.42, 0.52 and 0.58 have been synthesized by solid state reaction using high temperature. The compositions have been labelled PZTF-42 (corresponding to Zr/Ti = 42/58 and situated in the tetragonal region), PZTF-52 (corresponding to Zr/Ti = 52/48 and situated in the MPB region) and PZTF-58 (corresponding to Zr/Ti = 58/42 and situated in the rhombohedral region).

All the compositions have been obtained using high purity oxides (≥ 99%) like PbO, TiO_2, ZrO_2, and Fe_2O_3. The oxides powders were ball-milled for 10 h in ethanol, dried and calcined at 870°C for 4 h. The calcined powders were ball-milled again in ethanol for 10 h, dried, mixed with binder 5 wt% polyvinyl alcohol (PVA) solution and pressed in the discs form with 10 mm diameter. Discs have been sintered in air for 2 h at 1100°C, 1150°C, 1200°C and 1250°C using closed alumina crucible and a lead rich atmosphere ($PbZrO_3$). Experimental density of all sintered discs were measured by Archimedes method. The phases formation in the sintered discs were studied with X-ray diffractometer (XRD) using BRUKER AXS D8 Advance with CuKα radiation and Ni filter at room temperature. Microstructure and grain size were studied by scanning electron microscopy (SEM) using FESEM-FIB Workstation Auriga produced by Carl Zeiss, Germany. Before using for electrical measurements all the sintered discs have been electrode

on both sides by silver paste and fired at 650°C for 30 min. Relative dielectric constant (ε_r) and loss tangent (tan δ) were measured at room temperature at 1 kHz using LCR meter HM 8018. Ferroelectric hysteresis behaviour (P–E) of the un-poled discs were measured using the TF analyser 2000. To determine the piezoelectric properties, the sintered discs were poled in a silicon oil bath at 100°C for 30 minutes in a DC field of 3.5 kV/mm. Piezoelectric properties were determined after 24 h from polarization using impedance analyser 4294A by the resonance (f_r) and antiresonance (f_a) frequency method.

3 Results And Discussion

3.1. Sintering behaviour of the ferroelectric compositions

The addition of donor or/and acceptor dopants (like Fe^{3+}, Ni^{2+}, Mn^{2+}, Sb^{3+}, Nb^{5+}, etc.) in $Pb(Zr_xTi_{1-x})O_3$ system influences the microstructure and electrical properties of the compositions [11–13]. The final properties, obtained after sintering, depend on the value of the Zr/Ti ratio. Three new compositions have been studied. Thus the PZTF-42 composition corresponding to Zr/Ti = 42/58 is situated in the tetragonal region, PZTF-52 composition corresponding to Zr/Ti = 52/48 and situated in the MPB region and PZTF-58 composition corresponding to Zr/Ti = 58/42 and situated in the rhombohedral region.

By adding acceptor ions such as Fe^{3+} (for B site) in the $Pb(Zr_xTi_{1-x})O_3$ system (ABO_3), “hard” materials have been developed, according also to [14]. The introduction of Fe^{3+} ions as a dopant leads to oxygen vacancies.

The density of all studied sintered compositions has been determined based on Archimedes’ method. In order to increase the accuracy of the measurements, heavy samples have been used (> 3 g). In this paper the authors assume that the theoretical density of all studied PZT compositions is 8 g/cm^3. The results suggest (Table 1) that the relative density of all sintered sample was above 92% at least.

Table 1
Sintering behaviour of the compositions as a function of the sintering temperature

Sintering temperature T [°C]	Samples	Experimental density [g/cm^3]	Relative density [%]	Region
1100	PZTF-42	7.43	92.90	T
	PZTF-52	7.42	92.80	MPB
	PZTF-58	7.41	92.70	RH
1150	PZTF-42	7.47	93.40	T
	PZTF-52	7.48	93.50	MPB
	PZTF-58	7.47	93.40	RH
1200	PZTF-42	7.56	94.50	T
	PZTF-52	7.68	96.00	MPB
	PZTF-58	7.49	93.70	RH
1250	PZTF-42	7.65	95.70	T
	PZTF-52	7.72	96.50	MPB
	PZTF-58	7.57	94.70	RH

As reported in Table 1, for all the studied compositions the increase of the sintering temperature led to the increase of the density.

For all sintering temperatures, the best values are obtained for the PZTF-52 composition which is located in the MPB region.

3.2. Structural analysis

Figs. 1-4 show the experimental XRD patterns for each sintering temperature. X-ray diffraction patterns were acquired using a Bruker Axis D8Discover diffractometer, in Bragg-Brentano geometry, equipped with an Cu-Kα radiation tube and a LynxEye 1D detector, at a scan speed of 1s/step and incremental 2θ angle of 0.04^o.

All XRD patterns show the perovskite solid solution phase formation, with tetragonal structure. Splitting of (111) peak, at angular position of $2\theta \sim 38^o$, reveals an additional rhombohedral structure for PZTF-52 and PZTF-58 at lower temperature range (1100^{o}C-1200^{o}C). Since Fe^{3+} is known as a hard dopant, it is expected to replace Ti^{4+} or Zr^{4+} in B positions of the perovskite structure, therefore giving rise to a lattice distortion and appearance of structural vacation.

3.3. Electron microscopy studies

As from the Figs. 5–8, the microstructure of all sintered compositions is relatively homogeneous and fine grained, with an average grain size depending on the Zr/Ti ratio and the sintering temperature.

Samples sintered at 1100°C and 1200°C have been etched with a HCl and HF solution (5% HCl solution with 5 drops of HF per 100 cm3 of solution). SEM images at 50.00kX magnification for compositions sintered at 1100°C show a microstructure with pores and small grains distribution at the intergranular boundary of large grains (Figs. 5 (a-c)).

At 1150°C the SEM images (50.00kX magnification) are similar to the previous ones and show a microstructure with small granules, mostly placed at the limit of the large granules Figs. 6 (a-c). Also, a porosity of the samples was observed.

At 1200°C (Fig. 6–20.00kX magnification) and 1250°C (Fig. 7–20.00kX magnification) all compositions become much denser. The sintering temperature and the Zr/Ti ratio have a decisive role in obtaining the shape and size of the graines. Replacement of Zr^{4+} with Fe^{3+} leads to an increase in the grains size of the compositions [15].

In all cases, the MPB composition (PZTF-52) has a denser microstructure than the other two compositions located in the tetragonal region (PZTF-42) and rhombohedral region (PZTF-58).

It was found that the grains of different sizes are uniformly distributed in the all sintered compositions.

The decrease of the crystallites and the grain sizes could be due to the size mismatch of Fe^{3+} (0.64Ä) and Zr^{4+} (0.80Ä) ions, which creates a strain in the lattice. Fe-doping plays an important role in the control of grain growth, probably due to the oxygen vacancy formation, which could stop the grain boundary migration.

3.4. Ferroelectric characteristics

In Figs. 9–12 the ferroelectric hysteresis loops of all un-poled compositions sintered for 2 hours at 1100°C, 1150°C, 1200°C and 1250°C at room temperature are reported. It can be observed that all compositions sintered for 2 hours at sintered temperature shows hysteresis loops which are similar to the hysteresis loops of the hard materials [16, 17].

Domains reorientation are limited, and, all compositions are characterized by poorly developed hysteresis loops. The motion of domains walls influences the direction in which the electrical coercivity and remanent polarization are changing [18]. The presence of the domain walls is a result of multidomain structure of many ferroelectric crystals.

The motion of the domains walls is influenced by the grain size of the compositions and the type of vacancy defects [19, 20]. Very large grain size reduced the coercive field increas.

The remanent polarization reflects the internal polarizability of the material. Therefore, high is the remanent polarization, high is the polarizability of the material.

The values obtained for the remaining polarization (Pr) and the coercitive field (Ec) are in accordance with the results obtained by the SEM characterization.

3.5. Dielectric and Piezoelectric properties

At high sintering temperature, because of the decreasing of the number of pores, the dielectric and piezoelectric properties increase considerably associated to an enhanced domains walls mobility.

At 1100°C and 1150°C, the compositions could not be polarized. The structural inhomogeneity being the determining factor in this process. For the compositions sintered at 1200°C and 1250°C some results was reported elsewhere [21].

Table 2 presents the obtained values for the dielectric (loss factor (tan δ) at 1 kHz, relative dielectric constant (ε_r) at room temperature, Curie temperature (T_C) and resistivity (R_v)) and piezoelectric properties (the planar coupling factor k_p and the transversal coupling factor k_t) of the compositions PZTF-42, PZTF-52 and PZTF-58 sintered at 1250°C for 2h. The anisotropy has been determined by the ratio k_t/k_p.

To determine the Curie transition temperature, the dielectric constant was measured as a function of temperature at 1 kHz. The compositions show a typical ferroelectric phase transition peak at a Curie transition temperature higher than 445 ^oC.

It can be observed that all the values depend on the Zr^{4+}/Ti^{4+} ratio.

Table 2
The dielectric and piezoelectric properties for the all compositions sintered at 1250°C for 2h

Compositions	tan δ	ε_r	R_v *10^{17}(Ω*cm)	Tc [°C]	k_p	k_t	k_t/k_p
PZTF-42	0.0044	394	20.4	> 445	0.42	7.57	18.02
PZTF-52	0.0018	253	11.7	> 445	0.44	7.57	17.20
PZTF-58	0.0130	464	6.5	> 445	0.42	7.57	18.02

The anisotropy of poled compositions sintered at 1250°C is higher than 10, indicating a superior grade of alignment of the domains during poling. Densification and homogeneity of the ceramics are still the main factors of the improved piezoelectric properties.

4 Conclusions

In the present research paper, the ferroelectric compositions described by the general formula $Pb(Zr_xTi_{1-x})_{0.99}Fe_{0.01}O_3$ were synthesized by solid state reaction using high temperature. The dopant (Fe^{3+}) were diffused into the PZT lattice and all the sintered ferroelectric compositions revealed a good homogeneity. The results obtained indicate an influence of the Zr^{4+}/Ti^{4+} ratio on the dielectric and piezoelectric properties of the analysed compositions. The evolution of the grains size is directly associated to the sintering temperature and to the Zr^{4+}/Ti^{4+} ratio.

As for the dielectric and piezoelectric properties concern, it was observed that all the compositions sintered at 1100°C and 1150°C could not be polarized because of their structural inhomogeneity. The effects coming from the presence of high anisotropy piezo-active elements can be appropriately exploited for different applications, such as for the development of medical diagnostic devices or as promising target to be used as coating material.

Declarations

Acknowledgment:

The authors acknowledge the financial support of the Ministry of Research and Innovation, through PN 19310103/ 2019.

References

[1] Jaffe B, Cook WR, Jaffe H. Piezoelectric Ceramics. Academic Press, London and New York, 1971, 317.

[2] Swartz SL. Topics in electronic ceramics. *IEEE Trans Electr Insul* 1990, 25: 935–987.

[3] Kakegawa K, Mohri J, Takahashi T, *et al.* A compositional fluctuation and properties of Pb(Zr, Ti)O_3. *Solid State Commun* 1977, **24**: 769–772.

[4] Do DH. Investigation Of Ferroelectricity And Piezoelectricity In Ferroelectric Thin Film Capacitors Using Synchrotron X-Ray Microdiffraction, A dissertation submitted in partial fulfillment of the requirements for the degree of Doctor of Philosophy (Metallurgical Engineering) at the UNIVERSITY OF WISCONSIN-MADISON, 2006

[5] Qiu J, Ji H. Research on applications of piezoelectric materials in smart structures. *Front Mech Eng* 2011, **6**: 99–117.

[6] Noheda B, Cox DE, Shirane G, *et al.* A monoclinic ferroelectric phase in the $PbZr_{1-x}Ti_xO_3$ solid solution *Appl Phys Lett* 1999, **74**: 2059–2061.

[7] Noheda B, Cox DE, Shirane G, *et al.* Stability of the monoclinic phase in the ferroelectric perovskite $PbZr_{1-x}Ti_xO_3$. *Phys Rev B* 2000, **63**: 014103.

[8] Haertling GH. Ferroelectric Ceramics: History and Technology. *J Am Ceram Soc* 1999, **82**: 797–818.

[9] Wilson SA, Jourdain RPJ, Zhang Q, *et al.* New materials for micro-scale sensors and actuators. *Mater Sci Eng R Rep* 2007, **56**: 1–129.

[10] Turik AV, Topolov VYu. Ferroelectric ceramics with a large piezoelectric anisotropy. *J Phys D Appl Phys* 1997, **30:** 1541-1549.

[11] Miclea C, Tanasoiu C, Miclea CF, *et al.* Effect of iron and nickel substitution on the piezoelectric properties of PZT type ceramics. *J Eur Ceram Soc* 2005, **25**: 2397–2400.

[12] Moure C, Villegas M, Fernández JF, *et al.* Microstructural and piezoelectric properties of fine grained PZT ceramics doped with donor and/or acceptor cations. *Ferroelectrics* 1992, **127**: 113–118.

[13] Rai R, Mishra S, Singh NK. Effect of Fe and Mn doping at B-site of PLZT ceramics on dielectric properties. *J Alloys Compd* 2009, **487**: 494–498.

[14] Garcia JE, Pérez R, Albareda A, *et al.* Non-linear dielectric and piezoelectric response in undoped and Nb^{5+} or Fe^{3+} doped PZT ceramic system. *J Eur Ceram Soc* 2007, **27**: 4029–4032.

[15] Kahoul F, Hamzioui L, Boutarfaia A. The Influence of Zr/Ti Content on the Morphotropic Phase Boundary and on the Properties of PZT–SFN Piezoelectric Ceramics. *Energy Procedia* 2014, **50**: 87–96.

[16] Carl K, Hardtl KH. Electrical after-effects in $Pb(Ti, Zr)O_3$ ceramics. *Ferroelectrics* 1977, **17**: 473–486.

[17] Kamel TM, de With G. Poling of hard ferroelectric PZT ceramics. *J Eur Ceram Soc* 2008, **28**: 1827–1838.

[18] Morozov M, Damjanovic D, Setter N. The nonlinearity and subswitching hysteresis in hard and soft PZT. *J Eur Ceram Soc* 2005, **25**: 2483–2486.

[19] Warren WL, Pike GE, Vanheusden K, *et al.* Defect-dipole alignment and tetragonal strain in ferroelectrics. *J Appl Phys* 1996, **79**: 9250–9257.

[20] Warren WL, Vanheusden K, Dimos D, *et al.* Oxygen Vacancy Motion in Perovskite Oxides. *J Am Ceram Soc* 1996, **79**: 536–538.

[21] Dumitru AI, Clicinschi F, Dumitru TG *et al.* Effects of Sintering Temperature on Structural and Electrical Properties of Iron Doping PZT Ceramics, *Acta Marisiensis. Seria Technologica* 2020, **18**: 4-7.

Figures

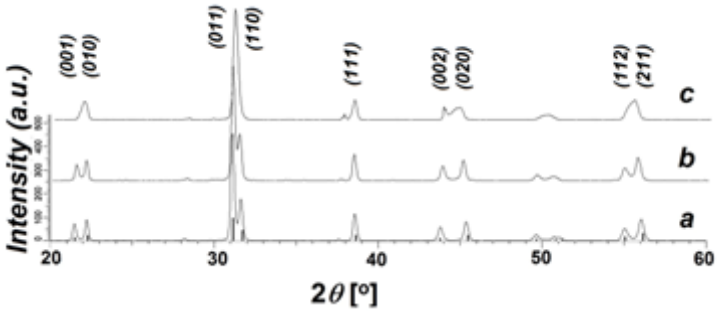

Figure 1

XRD patterns for (a) PZTF-42, (b) PZTF-52, (c) PZTF-58 at 1100°C

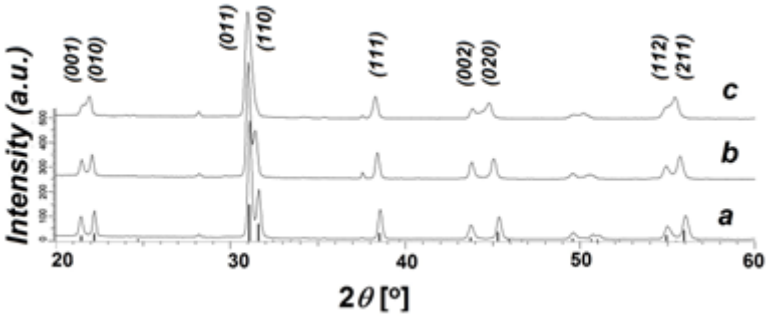

Figure 2

XRD patterns for (a) PZTF-42, (b) PZTF-52, (c) PZTF-58 at 1150°C

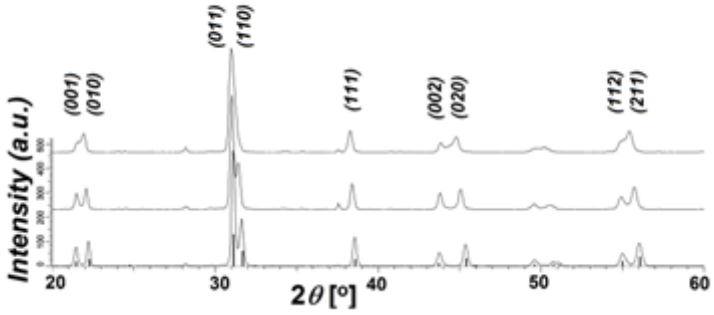

Figure 3

XRD patterns for (a) PZTF-42, (b) PZTF-52, (c) PZTF-58 at 1200°C

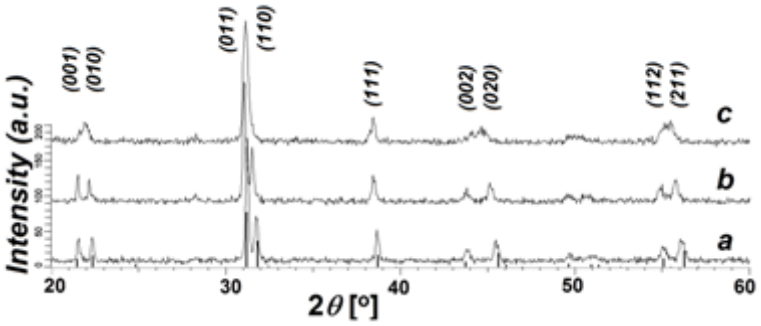

Figure 4

XRD patterns for (a) PZTF-42, (b) PZTF-52, (c) PZTF-58 at 1250°C

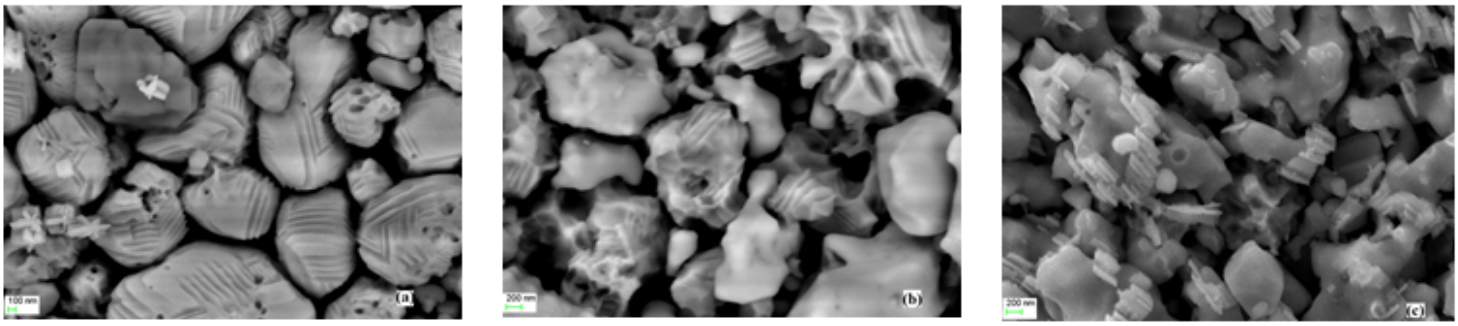

Figure 5

SEM images of the compositions thermally treated for 2 h at 1100°C (a) PZTF-42,(b) PZTF-52 and (c) PZTF-58

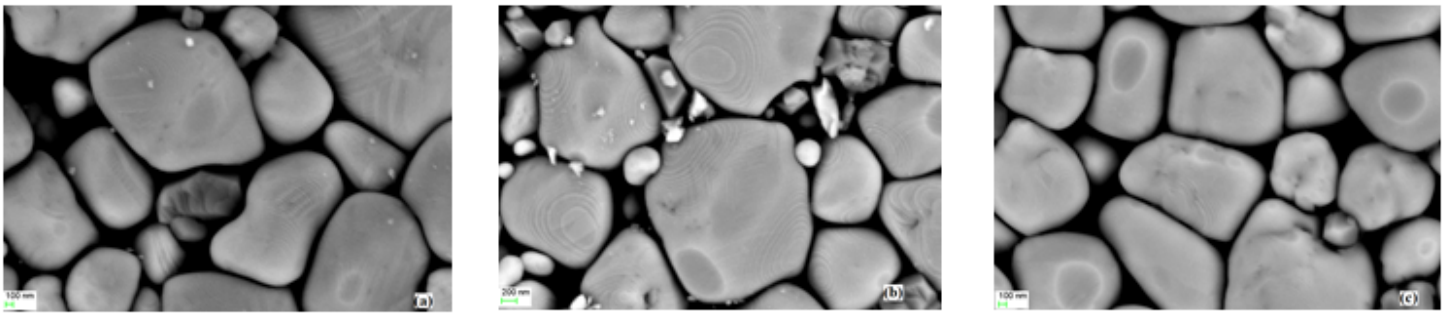

Figure 6

SEM images of the compositions thermally treated for 2 h at 1150°C (a) PZTF-42, (b) PZTF-52 and (c) PZTF-58

Figure 7

SEM images of the compositions thermally treated for 2 h at 1200°C (a) PZTF-42, (b) PZTF-52 and (c) PZTF-58

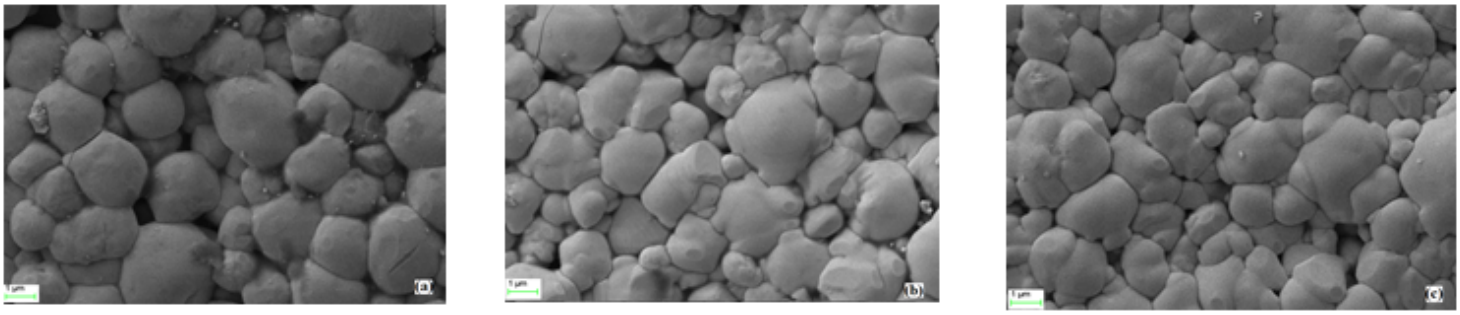

Figure 8

SEM images of the compositions thermally treated for 2 h at 1250°C (a) PZTF-42, (b) PZTF-52 and (c) PZTF-58

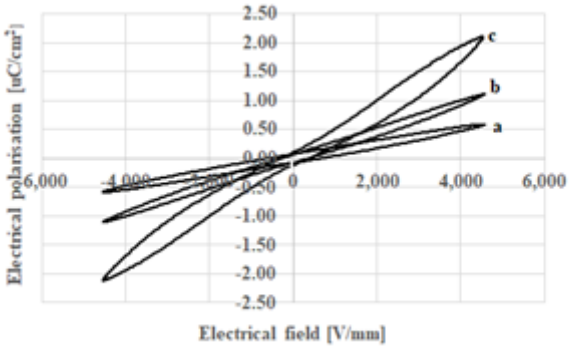

Figure 9

Room temperature ferroelectric hysteresis loops of compositions sintered for 2 h at 1100°C (a) PZTF-42, (b) PZTF-52 and (c) PZTF-58

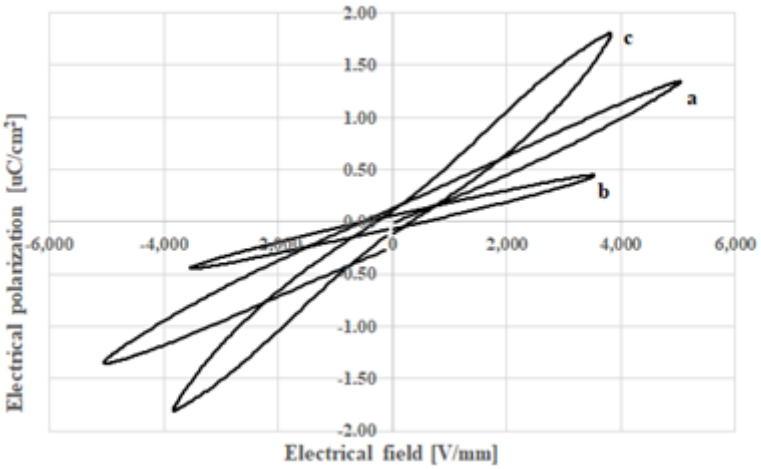

Figure 10

Room temperature ferroelectric hysteresis loops of compositions sintered for 2 h at 1150°C (a) PZTF-42, (b) PZTF-52 and (c) PZTF-58

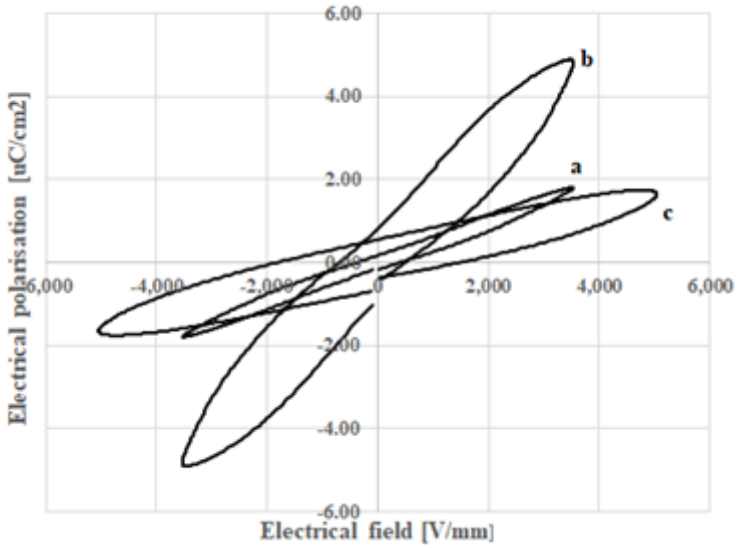

Figure 11

Room temperature ferroelectric hysteresis loops of compositions sintered for 2 h at 1200°C (a) PZTF-42, (b) PZTF-52 and (c) PZTF-58

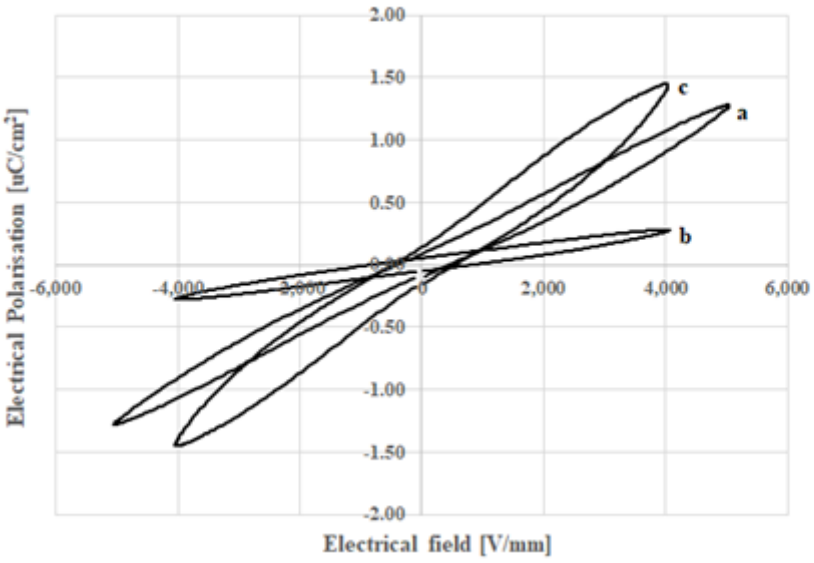

Figure 12

Room temperature ferroelectric hysteresis loops of compositions sintered for 2 h at 1250°C (a) PZTF-42, (b) PZTF-52 and (c) PZTF-58